Proc. Natl. Acad. Sci. USA
Vol. 92, pp. 11364–11367, December 1995
Colloquium Paper

This paper was presented at a colloquium entitled "Quasars and Active Galactic Nuclei: High Resolution Radio Imaging," organized by a committee chaired by Marshall Cohen and Kenneth Kellermann, held March 24 and 25, 1995, at the National Academy of Sciences Beckman Center, Irvine, CA.

The parsec-scale jet in M87

J. A. BIRETTA* AND W. JUNOR†

*Space Telescope Science Institute, 3700 San Martin Drive, Baltimore, MD 21218; and †University of New Mexico, Institute for Astrophysics, Albuquerque, NM 87131

ABSTRACT **We briefly review the observed structure and evolution of the M87 jet on scales ≤1 parsec (pc; 1 pc = 3.09 × 10^{16} m). Filamentary features, limb-brightening, and side-to-side oscillation are common characteristics of the pc-scale, and kpc-scale jets. The most prominent emission features on both the pc and subpc scales appear stationary ($v/c < 0.1$). Nonetheless, based on the jet's flux evolution, the presence of kpc-scale superluminal motion, and the absence of a visible counter-jet, we argue for the presence of an underlying relativistic flow, consistent with unified models. The initial jet collimation appears to occur on scales <0.1 pc, thus favoring electromagnetic processes associated with a black hole and accretion disk.**

The galaxy M87 contains the nearest powerful extragalactic jet in the northern hemisphere, and, thus, it is an ideal target for studying jet structure and evolution at high linear resolution. M87 is a giant elliptical and is one of two dominant galaxies in the Virgo Cluster. Fanaroff and Riley (1) classify it as a type I source (FR-I) on the basis of its radio morphology, though its luminosity ($P_{178\ \mathrm{MHz}} = 1.0 \times 10^{25}$ W·m^{-2}) places it near the FR-I/FR-II division. On arcsecond scales, it displays a well-collimated, one-sided jet, 2 kiloparsecs (kpc; 1 pc = 3.09 × 10^{16} m) in length which has been studied in detail from radio to x-ray frequencies (compare ref. 2, and references therein). On larger scales, radio images reveal two-sided structure extending to about 30 kpc.

Recent Hubble Space Telescope (HST) observations show the presence of a circumnuclear disk of ionized gas oriented normal to the jet as seen on the sky plane. Spectroscopic studies of this gas indicate the presence of a large mass, 2.4 × 10^9 solar masses, within the central 18 pc of the galaxy, which can be taken as evidence for the presence of a supermassive black hole (3, 4).

The distance to M87 ($z = 0.004$) has been determined to be 16 Mpc by using redshift-independent methods (5), which implies a linear scale of 0.078 pc per milliarcsecond (mas). Motions at 1 mas/year correspond to $0.254c$, where c is the velocity of light.

Jet Structure

The nucleus of M87 was among the first sources to be studied with very-long-baseline radio interferometry (VLBI) techniques (6, 7). Early 18-cm VLBI images (8) revealed a typical one-sided core jet morphology which was well aligned with the kpc-scale jet. Later observations with more antennae and better resolution (Fig. 1; ref. 9) revealed a 15-pc-long jet having a wealth of complex structure. The jet's brightness falls off fairly smoothly with distance from the core, although three prominent features (N2, N1, and L) stand out above the smooth emission.

"Filamentary" or narrow elongated structures can be traced along much of the jet in Fig. 1. For example, a linear feature can be traced along the northern limb between core distances $r \approx 40$ and ≈ 50 mas, at which point it appears to cross the southern limb, and then to cross back to the northern limb at $r > 65$ mas. Much of the jet also appears to be "limb-brightened" in that one or both edges are brighter than the jet center. For example, at 40 mas from the core, the jet is brightest along both edges and weaker along its centerline. At 65 mas, the jet is similarly bright at both edges. In other places, for example at 50 and 75 mas from the core, the jet appears bright only along the northern limb. The brightness centroid of the jet also appears to oscillate from side to side. Many of these characteristics can be interpreted in terms of helical, filamentary structures within the jet or wrapped around its surface (10–12).

Global VLBI observations at 22 GHz show that these characteristics continue down into sub-parsec scales (13, 14). Fig. 2*A* shows a tapered image with a resolution of ≈1 mas. Filamentary structure, limb-brightening, and side-to-side oscillation are again evident. The full resolution image (Fig. 2*B*) also shows evidence of oscillation and linear features, though the dynamic range is somewhat poorer than the tapered image. Evidence of filamentary features, limb-brightening, and side-to-side oscillation is also seen in the kpc-scale jet (12); these characteristics is present on scales from 0.1 to 1000 pc.

The jet appears to be well collimated on scales from <1 pc to several kpc, and there is a systematic trend for the jet's opening angle to decrease with core distance. Models fit to the (u, v) data of Fig. 2*B* within 0.1 pc of the core give a full-width-quarter-maximum opening angle of $\phi \approx 23° \pm 8°$, while Fig. 2*A* indicates a value near 13° at 1.5 pc. Farther out, we find $\phi \approx 9°$ at tens of pc (Fig. 1), and $\phi \approx 6°$ at 1 kpc. It is also interesting to consider the location of the jet's origin, as defined by the cone's apex on the smallest scales. If we extrapolate the brightness peaks along the jet's edges shown in Fig. 2*A* back toward the core, we find that the cone's apex lies within about 1 mas of the bright, unresolved core. Hence, in this simple picture of a cone with constant (or monotonically contracting) opening angle, the jet's initial collimation must take place on a scale smaller than about 0.1 pc.

Jet Evolution

The jet's kinematics appear to be complex on all scales. At the kpc scale, both stationary and superluminal features have been seen (15). The fastest features move outward at ≈$2c$ and are

The publication costs of this article were defrayed in part by page charge payment. This article must therefore be hereby marked "*advertisement*" in accordance with 18 U.S.C. §1734 solely to indicate this fact.

Abbreviations: pc, parsec; VLBI, very-long-baseline radio interferometry; VLBA, very-long-baseline array; mas, milliarcsecond; FWHM, full-width, half maximum; FR-I and -II, Fanaroff–Riley class I or II source.

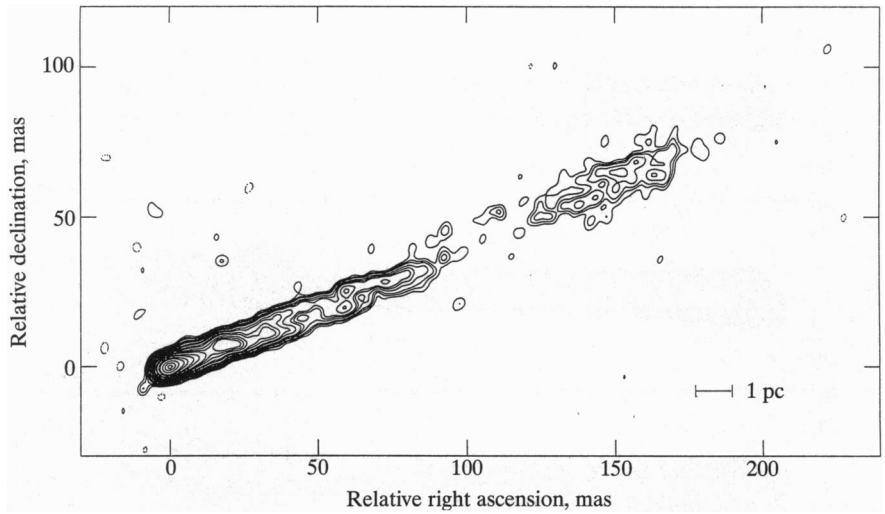

FIG. 1. Global VLBI image of M87 pc-scale jet at frequency 1.66 GHz from epoch 1984.26. The restoring beam is a 4-mas full-width, half maximum (FWHM) circular Gaussian function. The lowest contour is at 2 mJy·beam^{-1} (1 Jy = 10^{-26} W·m^{-2}·Hz^{-1}) (9).

located in knot D about 200 pc from the core, while other features in this knot, and also in knots B and C (1200–1500 pc from core), appear stationary (Table 1).

Fig. 3 shows a sequence of 18-cm images of the pc-scale jet. The two most prominent features, N1 and N2, both appear to be roughly stationary. Fig. 4 shows position measurements for N2. While the early data give evidence for outward motion at $\approx 0.3c$ (9), this motion does not continue at later epochs. Apparently, the position of N2 wanders by a few mas on timescales of a few years but is fixed on longer timescales. A linear fit to the data gives a speed $v/c = -0.03 \pm 0.02$, though it is a rather poor fit. Similarly, N1 has a very slow speed of $v/c = 0.02 \pm 0.04$.

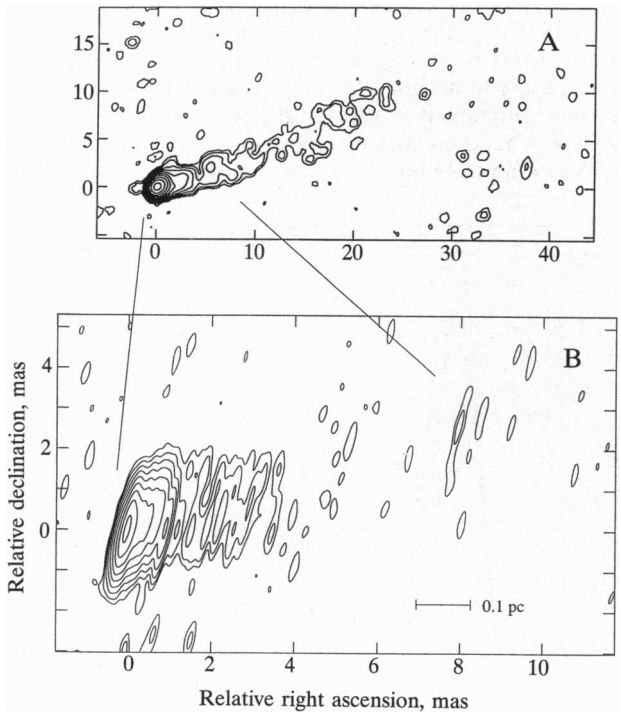

FIG. 2. Very-long-baseline array (VLBA) + European VLBI Network (EVN) image of M87 sub-pc-scale jet at 22 GHz from epoch 1992.87. North is up. Contours are at −2, −1, 1, 2, 4, 8, 16, 32, 64, 128, 256, and 512 mJy·beam^{-1}. (*A*) Image made from tapered (u, v) data; resolution 1.1 × 0.9 mas FWHM at position angle (PA) = −14°. (*B*) Full-resolution image with 1.3 × 0.14 mas FWHM at PA = −13° beam (14).

Careful examination of Fig. 3 also reveals many weaker features or local maxima in the brightness distribution. These features are very difficult to identify and track between epochs. They either change speed, flash on and off, or move large distances during the 4-year sampling period. For example, any features moving at $2.5c$, the highest speed seen in the kpc-scale jet, would travel the entire length of the visible pc-scale jet in only 8 years. It is natural to ask whether these weaker features merely reflect errors in the images. This seems unlikely; the contrast between these local maxima and the surrounding emission in many cases is 30 to 100 times the expected thermal noise (0.3 mJy). As with the pc-scale jet, the most prominent features in the sub-pc-scale jet also appear to be nearly stationary. Models fit to 22-GHz data at epochs 1992.45 and 1992.87 give speeds of $0.03c$ or less for features S2 and S3, both of which are within 0.04 pc of the core (Table 1).

Even though the prominent features are stationary in position, large flux variations are seen. Fig. 5 shows 18-cm brightness profiles along the jet at 8-mas resolution. Even though N2 is stationary, it appears to brighten by 60% between 1988 and 1992. In fact, the entire inner 30 mas of the jet brightens by amounts ranging from 20% to 60%. If this brightening is interpreted as the result of an outburst in the core, it implies an apparent propagation speed of at least $2c$ for the jet material. The available 22-GHz data also indicate 30% variations in the core and jet flux over 5 months (1992.45 to 1992.87).

As previously mentioned, the path of the jet shows evidence for side-to-side oscillation. It is interesting to ask whether the path of these oscillations is fixed or moves outward. The former result would suggest instability or external forces as the

Table 1. Apparent speeds for prominent features in M87 jet

Knot or feature	Core distance, pc	Apparent speed, v/c
C	1600	0.11 ± 0.04
A	970	0.509 ± 0.015
D–M	200	2.5 ± 0.3
N1	5	0.02 ± 0.04
N2	1.6	−0.03 ± 0.02
S3	0.04	0.03 ± 0.03
S2	0.013	0.01 ± 0.01

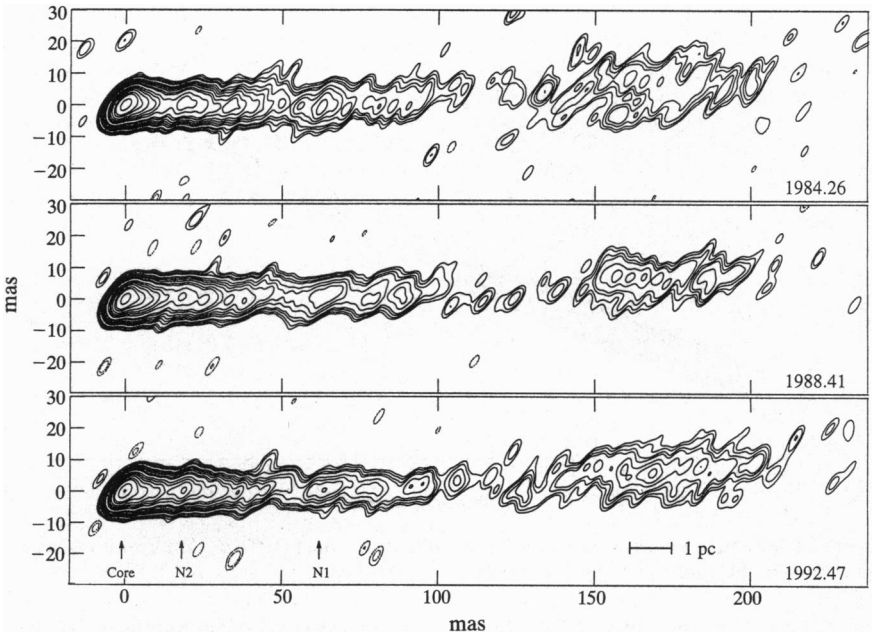

FIG. 3. Global VLBI images at 1.66 GHz for epochs 1984.26, 1988.41, and 1992.47. Prominent features N1 and N2 are labeled. All images have same 7.1 × 2.7 mas FWHM at PA = −13° Gaussian restoring beam. Contours are at −2, −1.4, 1.4, 2, 3, 4, 7, 10, 14, 20, 30, 40, 70, 100, 140, 200, 300, 400, 700, and 1000 mJy·beam^{-1}.

cause of the oscillations, while the later result would suggest precession-like effects. Examination of Fig. 3 shows a strong tendency for the oscillation pattern to remain fixed. For example, for r values between 25 and 40 mas from the core, the jet consistently runs south of the mean centerline. Similarly, the jet always runs north of the centerline for r values between 40 and 55 mas.

Discussion

Because of its proximity, M87 presents a unique opportunity to image an active galactic nucleus at small linear scales and, thus, to study the jet during its initial formation. From the 22-GHz observations, it is apparent that most of the jet collimation occurs on scales <0.1 pc, which corresponds to about 300 Schwarzschild radii for a putative 2×10^9-solar-mass black hole. Thus, it appears likely that the initial collimation is provided by electromagnetic processes which are tied to the black hole and accretion disk (16, 17). The interstellar medium might provide some collimation on larger scales (e.g., ref. 18) but is probably not the dominant agent.

One of the most interesting parameters of the pc-scale jet is the bulk-flow velocity. Models that attempt to unify the FR-I sources with BL Lacertae objects predict relativistic flows in the cores of FR-Is (19, 20). While there is no single piece of compelling evidence supporting relativistic flow in the core of M87, there is considerable circumstantial evidence for this. Superluminal motion (v up to 2.5c) is seen 200 pc from the core, which strongly suggests relativistic flow on those scales, and it is easy to imagine that flow originating in the nucleus. The most prominent features in the pc-scale jet appear to be stationary, but these may merely represent standing shocks or stationary obstructions in a rapid flow. The kpc-scale jet

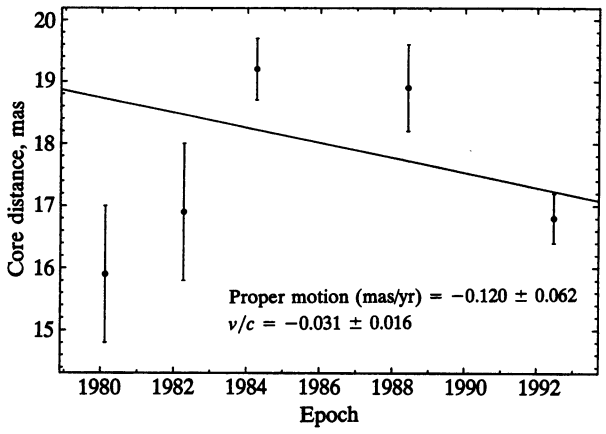

FIG. 4. Core distance vs. epoch for feature N2 in the pc-scale jet. Data are taken from 1.66-GHz VLBI images which are convolved to 8-mas resolution. The fitted line corresponds to motion at $-0.031c \pm 0.016c$.

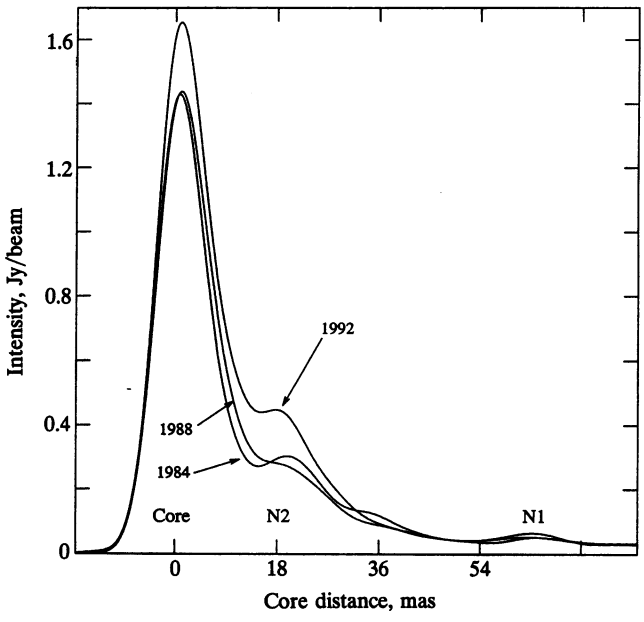

FIG. 5. Intensity as function of distance along jet at 1.66 GHz for three epochs.

displays superluminal features adjacent to stationary ones, such that one cannot dismiss the possibility of relativistic flow on the basis of the stationary features. The pc-scale jet also contains numerous features that cannot be tracked between available epochs, and rapid motion ($v_{apparent} > 2c$) is a viable explanation of their behavior. We have also seen that the inner 30 mas (2.4 pc) of the jet brightens in <4 years, which can be taken as evidence of flow at $>2c$. Finally, the usual limit on the jet/counter-jet brightness ratio (>150; ref. 9) implies flow with Lorentz $\gamma > 2$.

An alternate picture is one in which the pc-scale jet is slow but then accelerates between the pc and kpc scales. Such an acceleration might occur as the internal energy of a relativistic plasma is converted to bulk energy at a nozzle (21). However, the morphology of the jet and its opening angle are remarkably similar on these two scales. There is no obvious evidence for nozzle effects between these scales nor are there candidates for the site of such a nozzle, and other properties, such as the flux evolution and jet/counter-jet ratio, would still remain unexplained.

If one accepts that the M87 pc-scale jet contains a relativistic flow, it is interesting to ask why it is different from the BL Lacertae objects and quasars, in which the most prominent features are superluminal. A possible answer may lie in the orientation and limb-brightened appearance of M87. Constraints from motions in the kpc-scale jet and from the morphology of knot A together suggest the jet is oriented about $\theta \approx 43°$ from the line of sight (15). Deprojection of the circumnuclear gas disk also gives this orientation if one presumes the disk is normal to the jet (4). For such an angle, regions with bulk flow $\gamma \approx 3$ have no Doppler boosting, and, for larger γ, the emission is actually beamed away from the observer. We also note that the limb-brightened appearance suggests that much of the emission arises from the outer surface of the jet, where the external medium might cause instabilities and standing shocks, along with lower flow speeds. Hence, we have a picture in which M87 and its superluminal cousins may be intrinsically similar but appear different due to orientation effects: in M87 ($\theta \approx 43°$) the visible emission is dominated by slower material ($\gamma \lesssim 3$) near the jet's surface, where the speed and orientation give little Doppler beaming. Whereas in BL Lacertae objects and quasars ($\theta < 10°$) the visible emission is dominated by highly boosted material in a faster ($\gamma \gtrsim 5$), more coherent flow near the jet's center.

As the VLBA enters full operation, it should become possible to observe M87 at closely spaced epochs ($\lesssim$1-month intervals). This should greatly clarify the nature of the rapidly evolving features in the jet and show whether they in fact indicate relativistic flow in the nucleus. Future VLBI observations of M87 at millimeter wavelengths and by using Earth-orbiting antennae will further improve resolution and present a unique opportunity to image the "engine" within a few Schwarzschild radii of the putative black hole.

1. Fanaroff, B. L. & Riley, J. M. (1974) *Mon. Not. R. Astron. Soc.* **167,** 31–35.
2. Biretta, J. A. (1994) in *Astrophysical Jets*, eds. Burgarella, D., Livio, M. & O'Dea, C. P. (Cambridge Univ. Press, Cambridge, U.K.), pp. 263–304.
3. Harms, R. J., Ford, H. C., Tsvetanov, Z. I., Hartig, G. F., Dressel, L. L., Kriss, G. A., Bohlin, R. C., Davidsen, A. F., Margon, B. & Kochhar, A. K. (1994) *Astrophys. J.* **435,** L35–L38.
4. Ford, H. C., Harms, R. J., Tsvetanov, Z. I., Hartig, G. F., Dressel, L. L., Kriss, G. A., Bohlin, R. C., Davidsen, A. F., Margon, B. & Kochhar, A. K. (1994) *Astrophys. J.* **435,** L27–L30.
5. Tonry, J. L. (1991) *Astrophys. J.* **373,** L1–L4.
6. Cohen, M. H., Moffet, A. T., Shaffer, D., Clark, B. G., Kellermann, K. I., Jauncey, D. L. & Gulkis, S. (1969) *Astrophys. J.* **158,** L83–L85.
7. Kellermann, K. I., Clark, B. G., Cohen, M. H., Shaffer, D. B., Broderick, J. J. & Jauncey, D. L. (1973) *Astrophys. J.* **179,** L141–L144.
8. Reid, M. J., Schmitt, J. H. M. M., Owen, F. N., Booth, R. S., Wilkinson, P. N., Shaffer, D. B., Johnston, K. J. & Hardee, P. E. (1982) *Astrophys. J.* **263,** 615–623.
9. Reid, M. J., Biretta, J. A., Junor, W., Spencer, R. & Muxlow, T. (1989) *Astrophys. J.* **336,** 112–120.
10. Konigl, A. & Choudhuri, A. R. (1985) *Astrophys. J.* **289,** 173–187.
11. Hardee, P. E. (1987) *Astrophys. J.* **318,** 78–92.
12. Owen, F. N., Hardee, P. E. & Cornwell, T. J. (1989) *Astrophys. J.* **340,** 698–707.
13. Spencer, R. E. & Junor, W. (1986) *Nature* **321,** 753–755.
14. Junor, W. & Biretta, J. A. (1995) *Astron. J.* **109,** 500–506.
15. Biretta, J. A., Zhou, F. & Owen, F. N. (1995) *Astrophys. J.* **447,** 582–596.
16. Sakurai, T. (1987) *Publ. Astron. Soc. Jpn.* **39,** 821–835.
17. Li, Z.-Y., Chiueh, T. & Begelman, M. C. (1992) *Astrophys. J.* **394,** 459–471.
18. Wiita, P. J. & Siah, M. J. (1986) *Astrophys. J.* **300,** 605–612.
19. Browne, I. W. A. (1983) *Mon. Not. R. Astron. Soc.* **204,** 23–27.
20. Urry, C. M., Padovani, P. & Stickel, M. (1991) *Astrophys. J.* **382,** 501–507.
21. Daly, R. A. & Marscher, A. P. (1988) *Astrophys. J.* **334,** 539–551.